# Specific Absorption Rate Values of Handsets in Cheek Position at 835 MHz as a Function of Scaled Specific Anthropomorphic Mannequin Models

Ae-Kyoung Lee, Hyung-Do Choi, Jae-Ick Choi, and Jeong-Ki Pack

*ABSTRACT—A specific anthropomorphic mannequin (SAM) model was used to investigate the relation between local specific absorption rate (SAR) and head size. The model was scaled to 80 to 100% sized models at intervals of 5%. We assumed that the shell of the SAM model has the same properties as the head-equivalent tissue. Five handsets with a monopole antenna operating at 835 MHz were placed in the approximate cheek position against the scaled SAM models. The handsets had different antenna lengths, antenna positions, body sizes, and external materials. SAR distributions in the scaled SAM models were computed using the finite-difference time-domain method. We found that a larger head causes a distinct increase in the spatial peak 1-voxel SAR, while head size did not significantly change the peak 1-g averaged-SAR and 10-g averaged-SAR values for the same power level delivered to the antenna.*

*Keywords—SAM, handset, head size, SAR, FDTD technique.*

## I. Introduction

Different phone models, head models, and test positions have been used in many studies to investigate the effects of head size on specific absorption rate (SAR) [1]-[5]. Gandhi et al. [1] first published that smaller children's heads absorb more energy and have deeper penetration. Schönborn et al. [2] were not able to confirm the results. The controversy has sparked many studies [3]-[5]. Comparing the methods of [1] and [2], [1] used a fixed conducted power while [2] used a fixed current of the phone. A recent paper [3] compared the SAR results for both the constant current and conducted power, and concluded that the trend in the SAR values could be explained with the variation of the input resistance of the phone antenna. We previously studied the correlation between human head size and SAR characteristics for handset exposure using an anatomical model and a simple homogeneous model without the pinna attached [4], [5].

In this letter, we report the relation between head size and peak SAR values from a more general standpoint using various phone models with different electromagnetic characteristics, the specific anthropomorphic mannequin (SAM) head model, and the test position of IEEE Std 1528 [6]. The finite-difference time-domain (FDTD) method was used with sixteen perfectly matched layers, and all models were discretized with the uniform grid of $1 \times 1 \times 1$ mm$^3$. The spatial peak SAR values over 1 voxel, 1 g, and 10 g, and the current and voltage amplitudes at the antenna terminal of each phone model were calculated and compared.

## II. Numerical Models

The phone models of Fig. 1 are composed of a monopole and a body in the shape of a box. Their antennas are different in length, position, and/or covering material. Phone A, Phone B, and Phone C are the same in body size, material, and antenna position, but the antennas are different in length. The difference between Phone D and Phone B is that the rubber of the monopole in Phone B is removed and its plastic body is replaced with a perfect electric conductor (PEC). The monopole antenna of Phone E is located at the corner on top of the body and is not covered by other material as shown in

Manuscript received Nov. 22, 2004; revised Feb. 28, 2005.

This work was supported by Korea Ministry of Information and Communication.

Ae-Kyoung Lee (phone; +82 42 860 4971, email: aklee@etri.re.kr ), Hyung-Do Choi (email: choihd@etri.re.kr), and Jae-Ick Choi (email: jichoi@etri.re.kr) are with Digital Broadcasting Research Division, ETRI, Daejeon, Korea.

Jeong-Ki Pack (email: jkpack@cnu.ac.kr) is with the Department of Radio Science and Engineering, Chungnam National University, Daejeon, Korea.

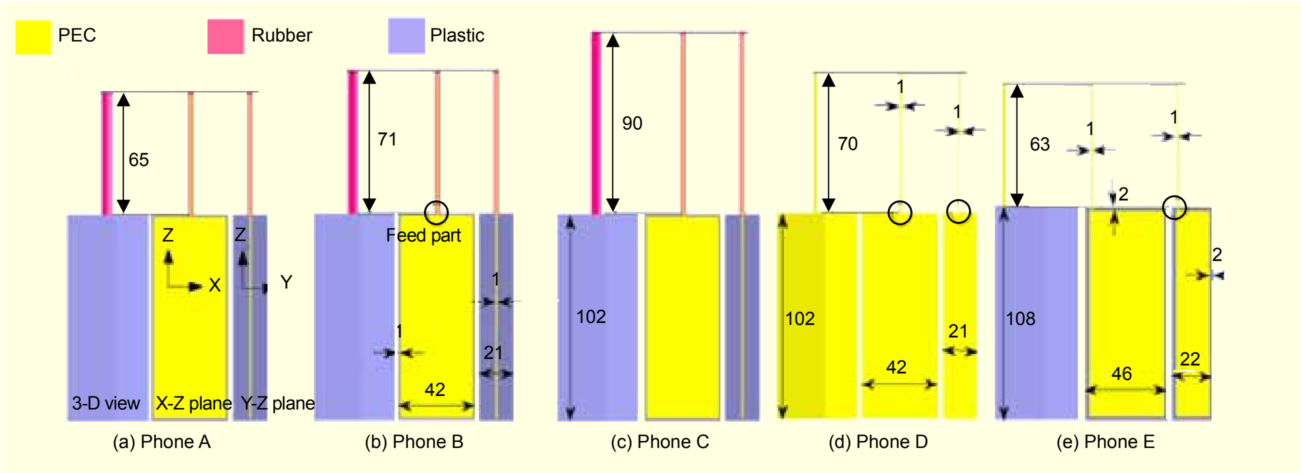


Fig. 1. Phone models.

Fig. 1. The electrical properties of the materials which cover the phone body and antenna are $\varepsilon_r$=4.0, σ=0.04 (S/m) and $\varepsilon_r$=2.5, σ=0.005 (S/m), respectively. Each acoustic output of the phones is assumed to be located at 1 cm below the top of the surface of the phone body.

Figure 2 represents the scaled head models based on a SAM model used for the standardized SAR measurement procedure of [6]. The SAM model generally offers better repeatability with respect to the test position of a phone than anatomical models. Both pinnae are a part of the shell in the SAM phantom and are not tissue-simulating material. The entire shell was assumed to be made from the same lossy material with tissue-equivalent properties in order to simulate a real pressed ear. Therefore, the 100% SAM in this letter is the same as the outer size of the original SAM shell. The head models are in a size range of 80 to 100% at intervals of 5%. The relative permittivity of 41.5, conductivity of 0.90 (S/m), and mass density of 1000 (kg/m$^3$) given in [6] were used for the FDTD simulation at 835 MHz.

We have chosen the cheek position described in [6] as the most usual test position of the phone models. The positioning process in virtual space is as follows. After positioning the phone model close to the right side surface such that the phone acoustic output is on the virtual line passing through the points, right ear (RE) and left ear (LE) of the phantom, translate the phone model towards the phantom along the virtual line until just before any voxel of the phone model collides with that of the head model, as shown in Fig. 3(a). Then, the phone model is rotated about its $Y^0$-axis until the vertical centerline is in the reference plane of the head model. The rotated angle becomes 61° counterclockwise. Figure 3(b) represents this position. Finally, the phone is rotated counterclockwise about the $X^1$-axis of the phone until any point of the phone model is in contact with the cheek of the SAM. The rotated angle becomes 6° clockwise. The relation between the coordinate system

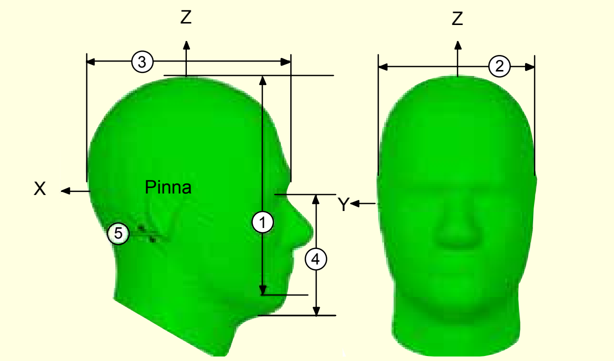


| Anatomy | 100% SAM model (mm) |
|---|---|
| ① Chin-top | 234 |
| ② Head breath | 162 |
| ③ Head length | 210 |
| ④ Menton-sellion | 129 |
| ⑤ Pinna thickness | 11 |

(a) Outer shape and size of 100 % SAM model.

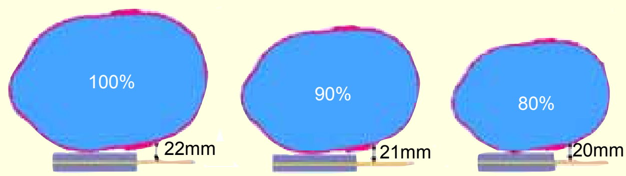


(b) Distance between antenna and the upper point of the pinna of the head

Fig. 2. Head models.

$[X^0\ Y^0\ Z^0]^T$ and the final coordinate system $[X^2\ Y^2\ Z^2]^T$ of Fig. 3 is represented as follows:

$$\begin{aligned}\left[X^2Y^2Z^2\right]^T &= {}^2_0R\cdot\left[X^0Y^0Z^0\right]^T\\ &= {}^2_1R\cdot{}^1_0R\cdot\left[X^0Y^0Z^0\right]^T\\ &= \mathrm{Rot}\left(X^1,-6^\circ\right)\cdot\mathrm{Rot}\left(Y^0,61^\circ\right)\cdot\left[X^0Y^0Z^0\right]^T\end{aligned}$$

$$\begin{bmatrix} X^2 \\ Y^2 \\ Z^2 \end{bmatrix} = \begin{bmatrix} 1 & 0 & 0 \\ 0 & c(-6^\circ) & s(-6^\circ) \\ 0 & -s(-6^\circ) & c(-6^\circ) \end{bmatrix} \cdot \begin{bmatrix} c61^\circ & 0 & -s61^\circ \\ 0 & 1 & 0 \\ s61^\circ & 0 & c61^\circ \end{bmatrix} \cdot \begin{bmatrix} X^0 \\ Y^0 \\ Z^0 \end{bmatrix},$$

where 'c' and 's' indicate cosine function and sine function, respectively.

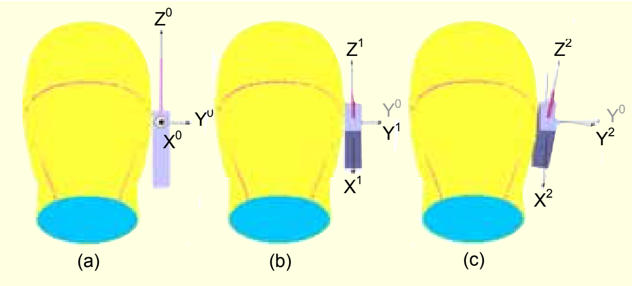

Fig. 3. Rotation process for cheek position.

## III. Results and Discussion

Spatial peak 1-voxel SAR, 1-g SAR, and 10-g peak SAR values for 25 cases of five phones and five head sizes were analyzed. Figure 4 represents spatial peak SAR results normalized to the maximum value when each phone antenna was fed 1.0 W, which is exclusive of the reflect power. For all the phones, the peak 1-voxel SAR is increased for the larger head. The rate of increase varies by phone, the average being about 12%. The positions of peak 1-voxel SARs vary partially with the phones and head size. On the other hand, while the peak 1-g SAR and 10-g SAR become decreased gradually in a larger model, the differences are insignificant, the positions being similar for all models. The average differences are about 2.5% and 2.6% for 1-g SAR and 10-g SAR in 80 to 100% sized head models, respectively. This trend is a little bit different from that in [3] and [4]. This is probably due to the closer distance between a smaller head and its phone, which is caused by the thinner ear scaled down in the same ratio with the head size.

Table 1 shows the input impedances of each phone antenna in cheek position. We can see that all the resistances and most of the reactance values of the phone models grow with the increase of head size. The increased resistance means that a larger head size results in an increase of voltage or decrease of current at the antenna feed part for the same power. Figure 5 represents the current and voltage normalized by the maximum value of each phone for the same antenna power. The antenna currents were decreased consistently as the head size grows, while the voltages were partially irregular. If the antenna current is fixed as in [2], the peak 1-g and 10-g SARs will be relatively increased in a larger head model.

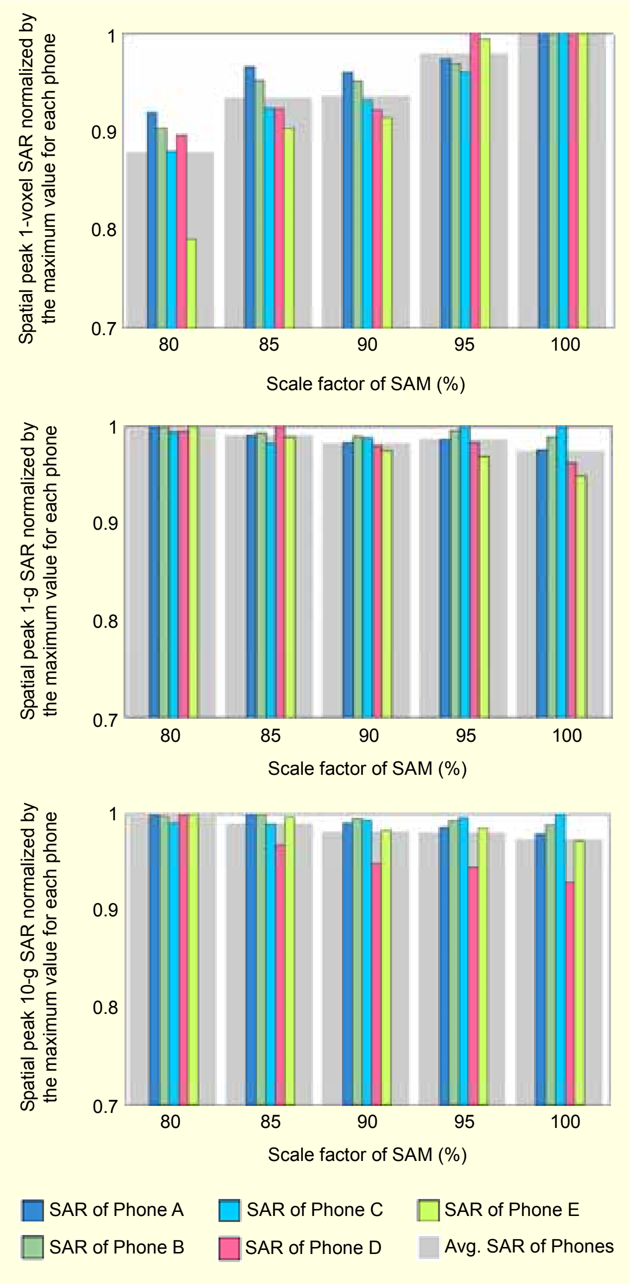

Fig. 4. Normalized peak SARs for the same antenna power.

## IV. Conclusions

SAR values in the modified SAM were compared with those in the reduced models when the delivered power to each phone antenna was constant. The results show that the peak 1-voxel SAR has an average difference of over 10% for 80 to 100% scaled SAM models, but 1-g SAR and 10-g SAR have a little difference of less than 3% between the head models.

The increasing trend in real impedance of the phones for the

Table 1. Input impedances of phone antennas under the cheek position.

(unit : Ω)

| Head models | Phone A | Phone B | Phone C | Phone D | Phone E |
|---|---|---|---|---|---|
| 80% SAM | 75.74−j40.18 | 84.09−j20.78 | 126.96+j49.76 | 39.84−j68.20 | 39.58−j65.93 |
| 85% SAM | 78.49−j39.27 | 87.17−j19.76 | 132.59+j54.42 | 41.45−j67.53 | 41.19−j65.55 |
| 90% SAM | 80.53−j42.15 | 89.18−j22.96 | 134.07+j49.57 | 42.15−j68.51 | 41.68−j66.63 |
| 95% SAM | 82.64−j43.48 | 91.48−j24.37 | 137.07+j47.65 | 43.31−j68.86 | 42.81−j67.03 |
| 100% SAM | 83.96−j46.75 | 92.72−j27.96 | 137.43+j42.70 | 43.77−j70.08 | 43.05−j68.28 |

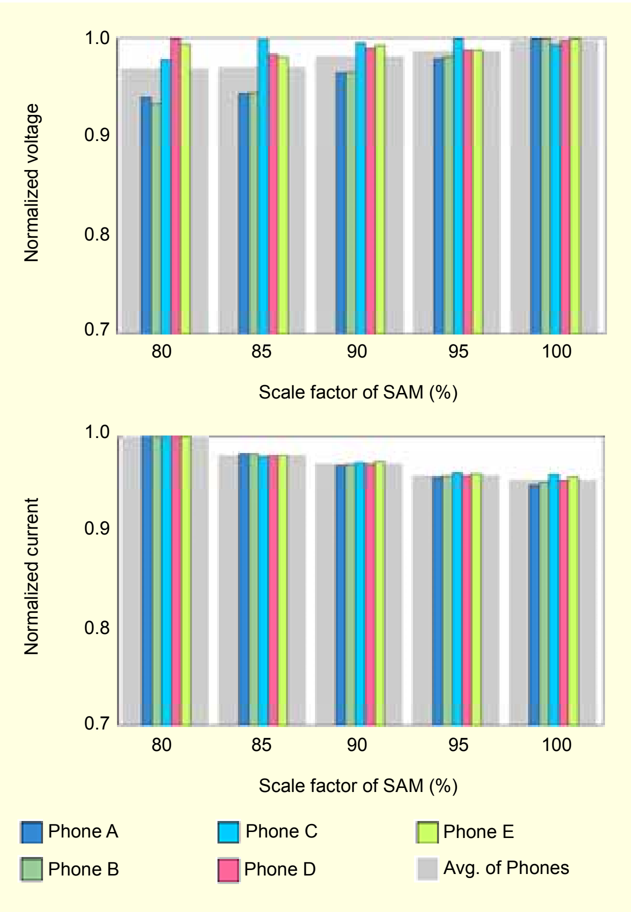


Fig. 5. Normalized antenna voltage and current for the same antenna power.

larger head model was observed similarly compared with the results in [3], in spite of the different head and phone models and test positions. However, a significant increasing of local SARs for a smaller head as in [1] was not observed in any case.

Although the models reduced evenly in all directions from the SAM model do not represent those of typical children or different races, we made sure that the results in this letter will offer useful data for the effects of head sizes on SAR, considering the pressed auricle and various bar-type phone models.

For SAR comparison, power delivered to each phone antenna was mainly used, but this power can be different from the output power of the phone in a real environment for wireless communication. From this point of view, the power radiated when using a phone is very important. A further study will be focused on the radiated power and pattern rather than the delivered power to a phone in an SAR comparison between children and adult mobile phone uses.

## Acknowledgement

The authors would like to thank IEEE SCC-34/SC-2/WG-2 who offered the SAM voxel model.

## References

[1] O.P. Gandhi, G. Lazzi, and C.M. Furse, "Electromagnetic Absorption in the Human Head and Neck for Mobile Telephones at 835 MHz and 1900 MHz," *IEEE Trans. Microwave Theory Tech.*, vol. MTT-44, no.10, Oct. 1996, pp.1884-1897.

[2] F. Schönborn, M. Burkhardt, and N. Kuster, "Differences in Energy Absorption between Heads of Adults and Children in the Near Field of Sources," *Health Physics*, vol. 74, 1998, pp.160-168.

[3] J. Wang and O. Fujiwara, "Comparison and Evaluation of Electromagnetic Absorption Characteristics in Realistic Human Head Models of Adult and Children for 900 MHz Mobile Telephones," *IEEE Trans. Microwave Theory Tech*, vol. MTT-51, no. 3, Mar. 2003, pp. 966-971.

[4] A.K. Lee and J.K. Pack, "Effect of Head Size for Cellular Telephone Exposure on EM Absorption," *IEICE Trans. Commun.*, vol. E85-B, no. 3, Mar. 2002, pp. 698-701.

[5] A.K. Lee, H.D. Choi, H.S. Lee, and J.K. Pack, "Human Head Size and SAR Characteristics for Handset Exposure," *ETRI J.* vol. 24, no. 2, Apr. 2002, pp. 176-179.

[6] IEEE Std 1528-2003, IEEE Recommended Practice for Determining the Peak Spatial-Average Specific Absorption Rate (SAR) in the Human Head from Wireless Communications Devices: Measurement Techniques, 2003.